Material Behaviour

Fabrication and characterization of isotropic magnetorheological elastomers

X.L. Gong*, X.Z. Zhang, P.Q. Zhang

CAS Key Laboratory of Mechanical Behavior and Design of Materials, Department of Mechanics and Mechanical Engineering, University of Science and Technology of China, Hefei 230027, China

Abstract

This paper presents a new method to fabricate isotropic magnetorheological (MR) elastomers under natural conditions. In the absence of a magnetic field, a variety of MR elastomer samples made of carbonyl iron particles, silicon rubber and silicone oil, were fabricated. Their dynamic viscoelastic properties were characterized by a measurement system developed by our group. Also, the microstructure of the samples was observed by a scanning electron microscope. The effects of iron particles and additives on the MR effect and the relationship between microstructure and mechanical properties were investigated. Furthermore, a simple self-assembled microstructure was proposed to explain the inherent magnetoviscoelasticity of MR elastomers prepared in the absence of a magnetic field. The analytical results of the model are in agreement with experimental data. The study is also expected to provide a good guide for designing and preparing new MR elastomers.
© 2005 Elsevier Ltd. All rights reserved.

1. Introduction

MR fluids (MRFs), discovered in 1948 [1], are a kind of colloidal suspension which can change their phase between liquid and solid under the control of a magnetic field. They are composed of oil with low permeability and micrometer sized ferrous particles. When a MR fluid is exposed to a magnetic field, the ferrous particles are magnetized and attracted by each other to form chains and columns in the direction of the external magnetic field, and the phase changes to solid. When it is sheared under a stress above its yield stress, it will show characteristics of the liquid phase again and the yield stress is determined by the external magnetic field. When the external field is removed, it will recover its phase from solid to liquid [2,3]. The quick response, good reversibility and controllable performance of MR fluids make them widely used in various devices, such

as dampers, clutches, and brakes [4–7]. However, MR fluids exhibit distinct shortcomings. For example, they are prone to particle settling with time due to density mismatch of particles and carrier fluid, which can degrade the MR effect. MR elastomers (MREs) are expected to overcome the disadvantages of MR fluids.

Structurally, MREs are analogs of MR fluids. They are also composed of micron-sized ferrous particles dispersed in a polymer medium. Conventionally, the mixture is cured in the presence of a magnetic field to fix the chainlike and columnar structures in the matrix. When such an anisotropic MRE is exposed to an external magnetic field, the elastic modulus will change with the intensity of the applied field [8]. The maximum modulus increase of MREs has been reported to be nearly 0.6 MPa (40% of initial modulus) when the iron volume concentration is 30% [9].

MRE can be used in many applications that employ variable stiffness, such as adaptive tuned vibration absorbers (TVAs), stiffness tunable mounts and suspensions, and variable impedance surfaces [10–13]. Ford Motor Company has patented an automotive bushing employing a MRE

---

* Corresponding author.
E-mail address: gongxl@ustc.edu.cn (X.L. Gong).

[10–11]. The stiffness of the bushing is adjusted according to the state of the automobile's power train to reduce suspension deflection and improve passenger comfort. Although currently there is little reported on applications of elastomers with controllable rheology, there is little doubt that there are numerous applications that can make use of controllable stiffness and others unique characteristics of these elastomers [13].

However, conventional methods to fabricate MREs under an external magnetic field have many shortcomings, which greatly limit their industrial application. Firstly, the conventional rubber-producing equipment must be modified to provide a magnetic field during crosslinking. Secondly, thick MREs cannot practically be fabricated because the magnetic flux density will decrease sharply as the thickness of the MRE increases. Thirdly, the chain direction of the anisotropic MRE must be considered when it is to be used in a particular device. However, according to current research, the anisotropic MREs have a much larger MR effect than that of isotropic MREs [14].

Some attempts have been tried to prepare isotropic MREs without external fields [15]. By using special particles and high particle volume concentration, the absolute MR effect in the isotropic MR rubbers is larger than that previously reported. However, these materials with such high iron particle concentrations have a high zero-field modulus so that the relative MR effect is quite low. Therefore, many challenges remain for the study of isotropic MREs.

This paper describes attempts to fabricate MREs under natural condition without an external magnetic field. Their dynamic performances were measured and compared with their microstructures. A simply self-assembled microstructure will be proposed to investigate such isotropic MREs.

2. Experimental

2.1. MRE sample preparation

The sample ingredients are carbonyl iron particles, silicone oil and 704 silicon rubber. The particles used were obtained from BASF and are spherical with an average diameter of 3 μm. The silicone oil has a viscosity of 0.1 PaS. Carbonyl iron particles were firstly immersed in silicone oil,

then they were mixed with 704 RTV silicone rubber. All the ingredients in the beaker were mixed by using a stirrer bar for about 5 min at room temperature. After all ingredients were evenly mixed, the mixture was put under a vacuum to remove air bubbles, and then cured for 24 h at room temperature in an open sheet mould without a magnetic field.

MR samples with different percentages of carbonyl iron particles, silicone oil and silicone rubber were prepared, as shown in Table 1. All these samples are classified into two groups. In group 1 (sample 1–4), the particle weight percentage of carbonyl iron particles was fixed at 60% (about 30% by volume.) and weight percentages of silicone oil were 0, 10, 20 and 30%, respectively. The residual percentage is silicone rubber. In group 2 (sample 5–8), the percentage of silicone oil was fixed as 20%, while the particle percentage ranges from 20 to 70%.

2.2. Mechanical property measurements

Mechanical properties of MR samples were measured using a system developed by our group, illustrated in Fig. 1. The dashed line shows the magnetic route, which is generated by an electromagnet system (Peking Excee-dlan Inc., China). The magnetic intensity is controlled by the electrical current intensity in the coil and measured by a Tesla gauge (model: CT3-A, made by Shangai No. 4 Electric Meter Factory, China) The induced magnetic field is imposed in the direction of the sample thickness. The MRE sample (30 mm in length, 10 mm in width and 6 mm in thickness), with its upper and lower surfaces adhered to two copper slabs, was inserted into the gap of the magnetic route. The upper slab was forced to vibrate by an exciter (JZQ-2), which was driven by a random signal source from a power amplifier whose signal was provided by a HP35665A Dynamic Signal Analyzer (Hewlett Packard Inc. in the USA) and a power amplifier (model: GF20-1, made by Baoying Baofei Vibration Instrument Factory in China). The vibrations of the two slabs were monitored by two identical piezoelectric acceleration transducers (CA-YD-103). The two signals from the transducers were input into two charge amplifiers (YE5858A, SINOCERA PIEZOTRONICS. INC. China), and then sent to the HP35665A Dynamic Signal Analyzer for processing and analysis.

Table 1
Composition of the samples (weight percentage)

Sample no.	Percentage of carbonyl iron particles (%)	Percentage of silicone oil (%)	Percentage of silicone rubber (%)	Sample No.	Percentage of carbonyl iron particles (%)	Percentage of silicone oil (%)	Percentage of silicone rubber (%)
1	60	0	40	5	20	20	60
2	60	10	30	6	40	20	40
3	60	20	20	7	60	20	20
4	60	30	10	8	70	20	10
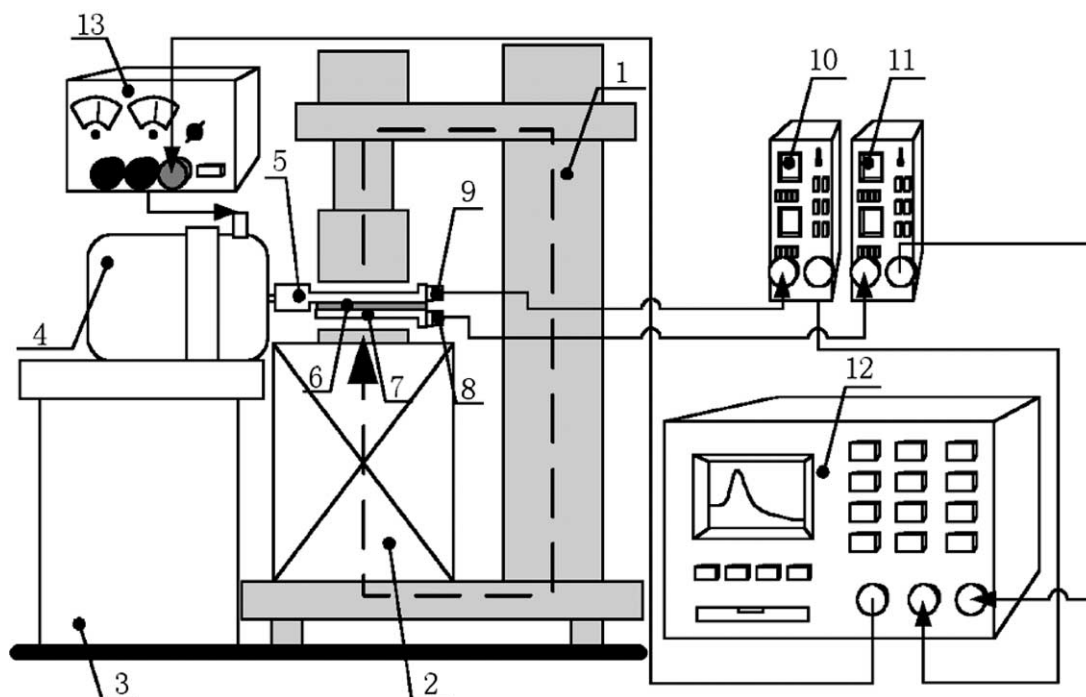
Fig. 1. Schematic of the performance testing setup: (1) magnetic route; (2) wire coils; (3) base; (4) exciter; (5) copper slab 2; (6) sample; (7) copper slab1; (8) acceleration transducer 1; (9) acceleration transducer 2; (10) charge amplifier1; (11) charge amplifier2; (12) HP35665A dynamic signal analyzer; (13) power amplifier.

MREs with the lower slab are modeled as a single degree of freedom system with a complex stiffness of $k_\tau(1 + i\eta)$, where k_τ, η are stiffness and loss factor, respectively. The stiffness can be given as $k_\tau = GA/h$, where A is the area of the sample's shear surface, h is the thickness and G is the shear modulus of MRE. The mechanical parameters of MREs can be identified from the following system transfer function

$$T(\omega) = \frac{k_\tau(1 + i\eta)}{-M\omega^2 + k_\tau(1 + i\eta)} \qquad (1)$$

where M is the effective mass and ω is the angle frequency. The transfer function is defined as from the ratio (i.e. transfer function) of the response signal (i.e. the lower transducer) to the excitation one (i.e. the upper transducer) in the frequency domain. The analyzer provides three columns of data. They are lists of frequency, and real and imaginary parts of the transfer function. The correlation coefficients of the signals from the two transducers can also be displayed on the analyzer. The minimum coefficient is about 0.97, so the reliability of the system is good enough. Substituting the data into Eq. (1), the mechanical parameters of MREs can be calculated by the data obtained from the HP35665A.

2.3. Microstructure observation

Microstructures of MR samples were observed by using a scanning electron microscope (SEM) (model: XT30

ESEM-TMP, Philips of Holland). This system can observe and analyze samples in their primitive state, even when containing water or oil. It provides the images of the samples that illustrate the microstructure of particles in the MREs.

3. Experimental results

For group 1 samples (sample 1–4) with various silicone oil contents from 0 to 30%, the transfer function in the frequency domain was measured at $B = 0$ and 200 mT by the above system. Substituting the transfer function into Eq. (1), the shear moduli of such samples at these magnetic fields were obtained. The results are shown in Fig. 2. The curves are composed of 400 data points from frequency 100 to 600 Hz. They are not fitted curves and so look somewhat scattered. The modulus changes with the frequency. To compare conveniently, only at the resonance frequency of every sample, the modulus change, ΔG, and the ratio, $\Delta G/G0$, were calculated and are summarized in Table 2. As shown in Table 2, the modulus ratio increased steadily until a maximum value of 26% at a silicone oil content of 20%. Above this oil content, it decreased. SEM images for these samples are shown in Fig. 3. For sample 1 without any silicone oil, the particles disperse randomly in the matrix, as shown in Fig. 3(a). When there is 20% of silicone oil
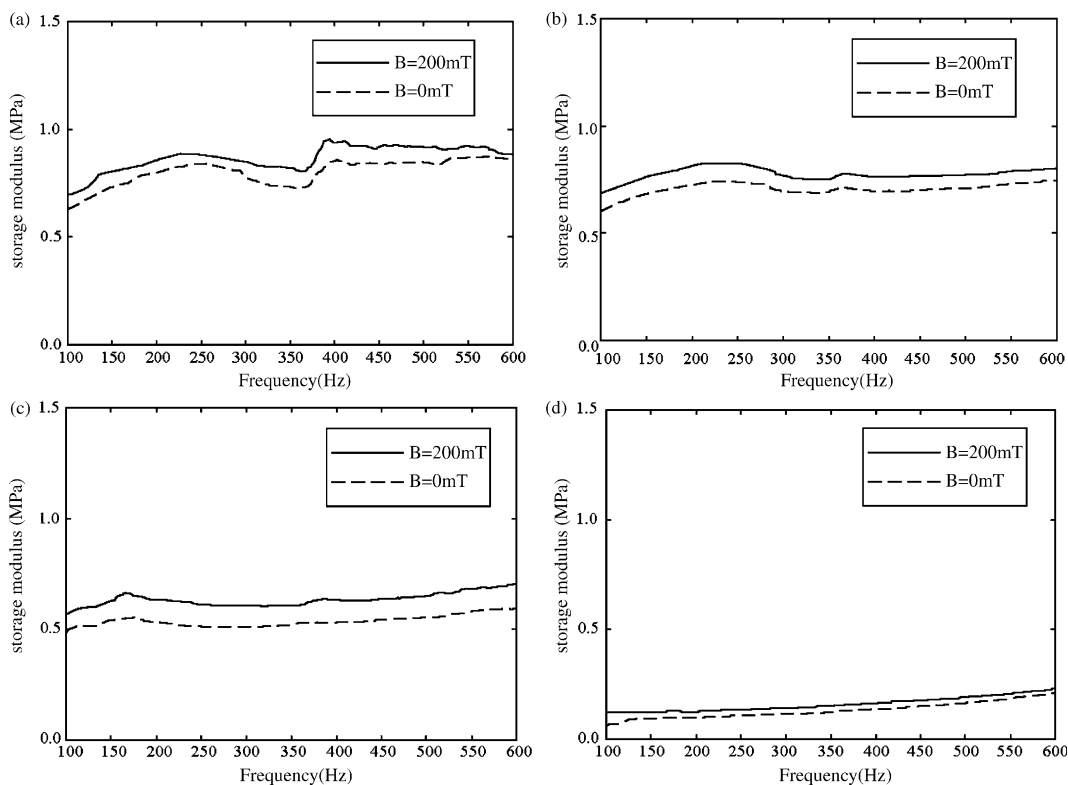
Fig. 2. Variation of shear modulus with frequency ($B=0$ and $B=200$ mT)—group 1 samples: (a) sample 1; (b) sample 2; (c) sample 3; (d) sample 4.

(sample 3), the particles in the sample attach to each other and form a partial microstructure, as shown in Fig. 3(c). This kind of microstructure is mainly composed of carbonyl iron particles with silicone oil between them, dispersed in the silicone rubber. When the sample is exposed to a magnetic field, the particles in the microstructure are magnetized and move slightly to form a more regular structure with the help of the lubrication of silicone oil, which consequently results in high MR effect. When the percentage of silicone oil is larger or smaller than 20%, the samples have less MR effect than the sample with 20% silicone oil. This is in agreement with Fig. 3. Comparing Fig. 3(b) and (c), it is found that the microstructure of sample 2 is less good than that of sample 3, whilst Fig. 3(d) shows that the matrix of sample 4 no longer has a fine rubber construction because it contains too much silicone oil. Therefore, 20% silicone oil gives the best condition to form a self-assembled microstructure, which results in the maximum MR effect.

Group 2 samples were used to study influence of particle content on the MR effect. The frequency dependence of shear moduli at $B=0$ and $B=200$ mT are shown in Fig. 4. Similarly, the variation of moduli between the two states are listed in Table 3 and their microstructures are shown in Fig. 5.

As shown in Table 3, the MR effect increases with increase in the percentage of carbonyl iron particles, except

that the variation of modulus of sample 8 changes differently with different frequencies. When the weight percentage of carbonyl iron particles is 20% (sample 5), there is no self-assembled microstructure in the sample. When the percentage of carbonyl iron particles reaches 40% (sample 6) the self-assembled microstructure can be seen clearly, as shown in Fig. 5(b). Again, when the percentage of carbonyl iron particles is 60% (sample 7) particles form a stable self-assembled microstructure. For sample 8, there is 70% carbonyl iron particles and the percentage of silicone rubber is only 10%. At this level the sample is very floppy and the toughness of the rubber is lost. Also, the microstructure shows many cracks and compound is not practically useful. Comparing all the samples of group 2, where the silicone oil content is fixed at 20%, sample 7 with iron particle content of 60% is found to have the best mechanical performance.

Table 2
Variation of shear modulus of group 1 samples (at the resonance frequency)

Sample no.	1	2	3	4
G_0 (Mpa)	0.85	0.75	0.53	0.15
ΔG (Mpa)	0.06	0.08	0.14	0.03
$\Delta G/G_0$ (%)	7	11	26	20
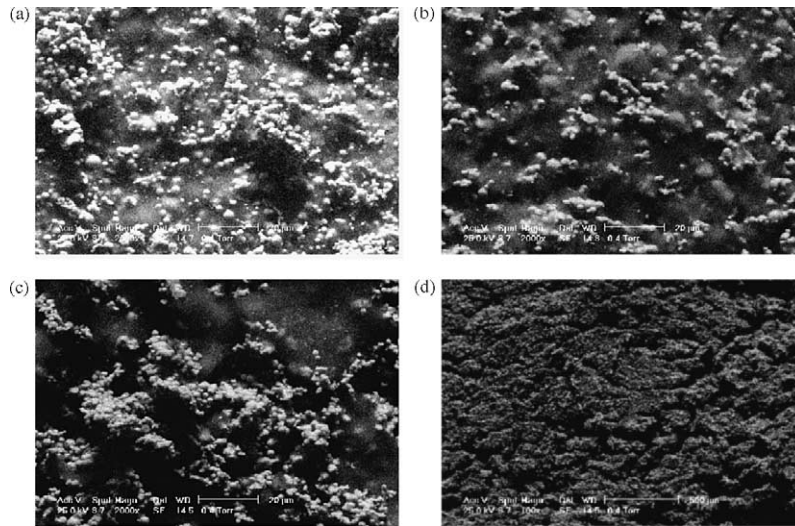
Fig. 3. Microstructures of group 1 samples: (a) sample 1; (b) sample 2; (c) sample 3; (d) sample 4.

The effects of magnetic field on the shear modulus of sample 7 are shown in Fig. 6(a). As can be seen, the modulus increases steadily with the increase of magnetic field. Fig. 6(b) shows the modulus versus magnetic flux density at the resonance frequency of 150 Hz. The relative modulus increase can reach roughly 60% when the flux density is 1.0 T, which is similar to the results of anisotropic MRE fabricated under a strong magnetic field [9].
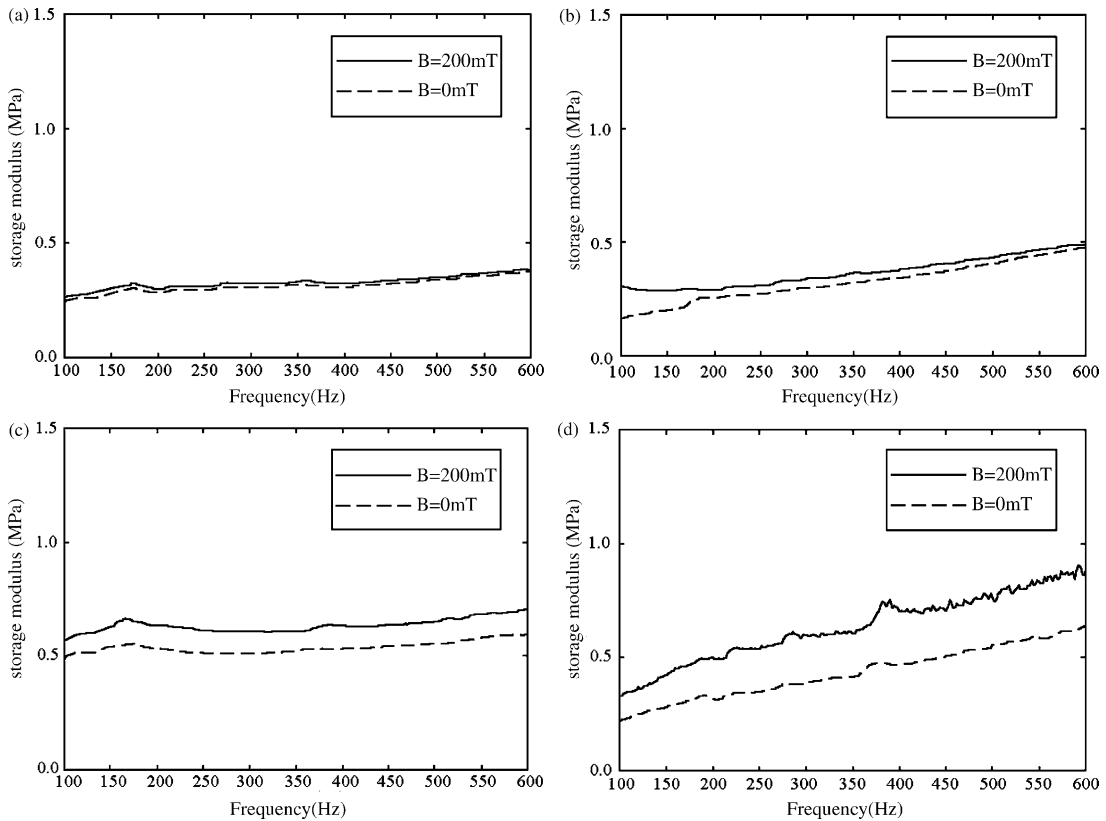
Fig. 4. Variation of shear modulus with frequency ($B=0$ and $B=200$ mT)—group 2 samples: (a) sample 5; (b) sample 6; (c) sample 7; (d) sample 8.

Table 3
Variation of shear modulus of group 2 samples (at the resonance frequency)

Sample no.	5	6	7	8
G_0 (MPa)	0.29	0.3	0.53	0.33
ΔG (MPa)	0.01	0.03	0.14	0.17
$\Delta G/G_0$ (%)	3	10	26	51

4. Modeling approach

During fabrication of MREs without the help of a magnetic field, carbonyl iron particles are mixed with silicon oil before they are blended with rubber material. The silicon oil helps the particles to attach to each other and self-assemble a partial microstructure. This is because of the surface tension of the additive. If the particles are spherical with the same particle size, they will probably form face-centered cubic (FCC) and hexagonal close packed (HCP)

microstructures. The SEM images have also supported this assumption.

To analyze the influence of the assembled structure on the absolute variation of shear modulus of this kind of isotropic MRE, a simple self-assembled model is proposed as shown in Fig. 7. For convenience of comparison, two kinds of structures with same particle size and same volume percentage of particles are considered as shown in Fig. 7(a) and (b), respectively. One proposed structure is shown in Fig. 7(a), where the particles disperse in the matrix as a lattice of single particles. In the figure, R is the radius of particle and d is the distance between two particles. The other structure is in Fig. 7(b). The particles firstly assemble a simple aggregation and then disperse in the matrix as a lattice of aggregated particles. For convenience of calculation, the aggregations are assumed to be composed of two particles and they aggregate in two directions, although there could be other microstructure and orientations in isotropic MREs. When the volume percentage is the same
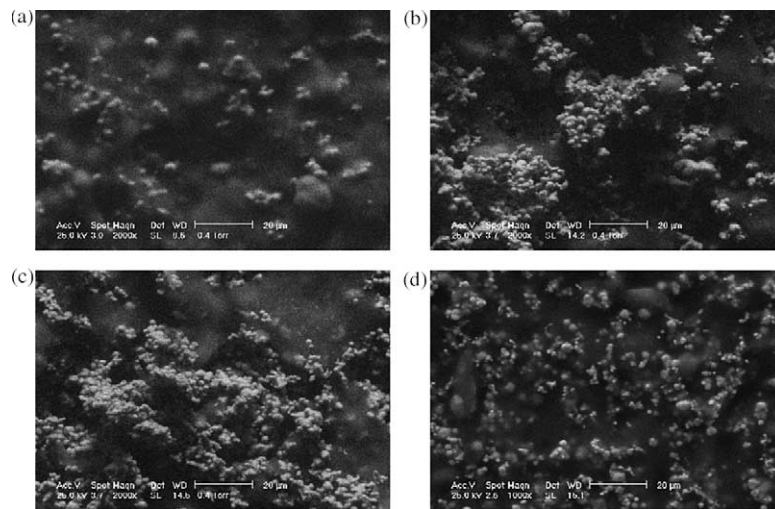
Fig. 5. Microstructures of group 2 samples: (a) sample 5; (b) sample 6; (c) sample 7; (d) sample 8.
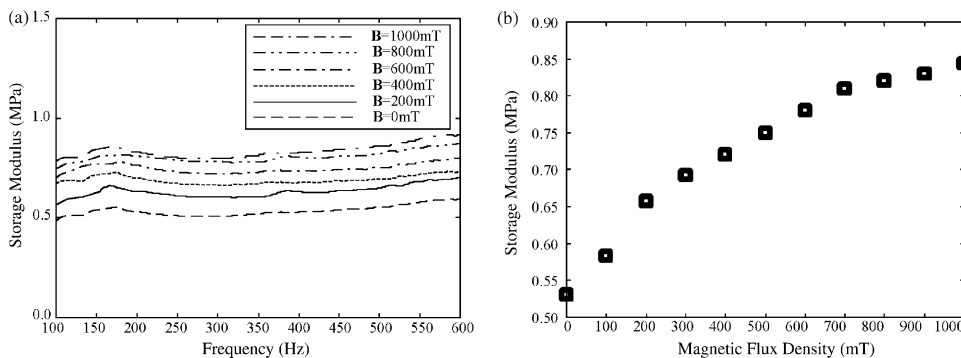
Fig. 6. Absolute MR effect of sample 7: (a) modulus versus frequency; (b) modulus versus applied magnetic field ($f=150$ Hz).
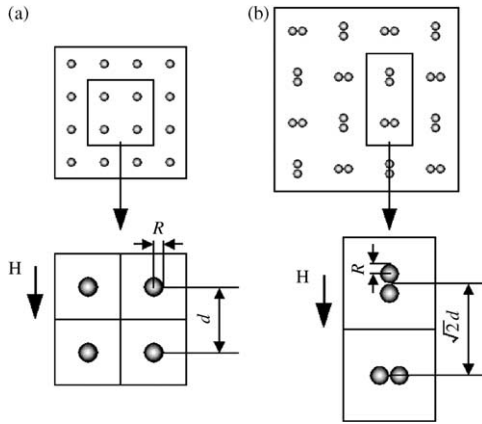
Fig. 7. Different distributions of particles in matrix: (a) lattice of particles; (b) lattice of a kind of simple particles' aggregation.

for both these two structures, the particle distance should be d and $\sqrt{2}d$, as shown in Fig. 7(a) and (b), respectively.

As shown in Fig. 7(a), the magnetic dipole moment of a particle under external field H_0 is

$$m_a = 4\pi\mu_m\mu_0 R^3 \beta H_0 \tag{2}$$

where μ_0 is the vacuum permeability, $\beta = (\mu_p - \mu_m)/\mu_p + 2\mu_m)$, μ_p is the relative permeability of particles and μ_m is the relative permeability of the matrix. For carbonyl iron particle and silicone rubber, $\mu_p \approx 1000$, $\mu_m \approx 1$ and $\beta \approx 1$.

The simple dipole model [16] predicts the maximum shear modulus is: $\Delta G = 4.808\phi\mu_0(R/d)^3 M_s^2$ where M_s is the saturation magnetization. Replacing the M_s with the magnetic dipole, the increase in the shear modulus ΔG_{da} can be expressed as:

$$\Delta G_{da} = 36\phi\mu_m\mu_0\beta^2 H_0^2 \left(\frac{R}{d}\right)^3 \zeta \tag{3}$$

where $\zeta = \sum_{k=1}^{\infty} \frac{1}{k^3} \approx 1.202$ denotes the influence of all the particles in a chain along the magnetic field direction.

The local field model [17] gives the horizontal and vertical components of magnetic dipole moment of a particle in a chain as

$$m_{\parallel} = \frac{4\pi\mu_f\mu_0 R^3 \beta H_0 \cos\theta}{1 - 4\beta\cos^3\theta\left(\frac{R}{d}\right)^3\zeta} \text{ and } m_{\perp} = \frac{4\pi\mu_f\mu_0 R^3 \beta H_0 \sin\theta}{1 + 2\beta\cos^3\theta\left(\frac{R}{d}\right)^3\zeta}$$

respectively, where θ is the angle between the chain and the magnetic field direction. As shown in Fig. 7(b), the magnetic dipole moment of the pair of particles in the upper aggregation (Two particles connect along the magnetic field direction) can be written as

$$m_{bu} = \frac{16\pi\mu_m\mu_0 R^3 \beta H_0}{2 - \beta} \tag{4}$$

The magnetic dipole moment of the pair of particles in the lower aggregation (Two particles connect

horizontally) is

$$m_{bl} = 8\pi\mu_m\mu_0 R^3 \beta H_0 \tag{5}$$

From the simple dipole model (regard the aggregation as a dipole), the increase in the shear modulus ΔG_{db} can be expressed as [16]:

$$\Delta G_{db} = \frac{36\sqrt{2}\phi\mu_m\mu_0\beta^2 H_0^2 \left(\frac{R}{d}\right)^3 \zeta}{2 - \beta} \approx 1.4\Delta G_{da} \tag{6}$$

Therefore, if the particles assemble together, the increase in the shear modulus due to the applied field will be improved. In other words, the self-assembled microstructure indeed improves the MR effect.

The self-assembled microstructure can also decrease the initial shear modulus. The initial modulus of MRE without magnetic field can be written as [16]:

$$G_e = G_0(1 + 2.5\Phi + 14.1\Phi^2) \tag{7}$$

where G_0 is the modulus of matrix and ϕ is the volume percentage of particles.

In the following, the particle volume percentage in the MRE is assumed to be 30%. From Eq. (7), if the particles are distributed in the matrix unattached, the initial modulus G_{e1} is $2.344G_0$. However, if the particles in the matrix are attached to each other and form a FCC or HCP construction, the initial modulus of the MRE will be calculated by the following two steps. At step 1, the aggregations with FCC or HCP construction have the modulus G_c as $10.6G_0$ because their volume percentage of particles is 74.1%. For step 2, these aggregations disperse in the matrix with a volume percentage of about 40.5%. The initial modulus G_{e2} of this kind of MRE can be calculated as $1.9G_0$ by Jiang's method [18]. Alternatively, by the approximate method of series springs, the modulus can be written as:

$$G_{e2} = \left(\frac{\phi_s}{G_c} + \frac{1 - \phi_s}{G_0}\right)^{-1} \approx 1.58G_0 \tag{8}$$

Whether using Jiang's method or the method of Eq. (8), it is obvious that $G_{e2} < G_{e1}$. Therefore, if the particles in MREs form a self-assemble microstructure, the initial modulus of MREs can be decreased remarkably. This also results in the increase of the relative MR effect.

However, if there is too much additive, the rubber will become too soft to sustain the load, with consequent decrease in modulus. Therefore, the appropriate percentage of additive is a key element to fabricate high-efficiency MREs. In summary, the key technique to improve the performance of MREs prepared without a magnetic field is to form a partial self-assembled microstructure.

5. Conclusions

Isotropic MREs were fabricated under natural conditions without an external magnetic field. Their performance

and microstructures were studied. It was found that the construction in such MREs is no longer chains or columns of particles. By the help of an additive, such as silicone oil, the particles form a kind of self-assembled microstructure in the MRE. This kind of microstructure is composed of additive and particles dispersed in the matrix. When this kind of MREs is exposed to a magnetic field, the particles in the microstructure are magnetized and move slightly by the lubrication of the additive to form a regular construction, which results in a high MR effect. Experiments show that when preparing such isotropic MREs by using carbonyl iron particles, silicone rubber and silicone oil, the MREs have the best MR effect when their percentages are about 60, 20 and 20%, respectively. The modulus enhancement can reach 60%, the same degree as for MRE fabricated under a strong magnetic field. Furthermore, a simple micro-assemble model is proposed to explain the MR effect, which is in agreement with the experimental data.

Acknowledgements

References

[1] J. Rabinow, AIEE Transactions 67 (1948) 1308–1315.
[2] J.D. Carlson, M.R. Jolly, Mechatronics 10 (2000) 555–569.
[3] W.H. Li, G.Z. Yao, G. Chen, S.H. Yeo, F.F. Yap, Smart Materials & Structures 9 (1) (2000) 95–102.
[4] B.F. Spencer, S.J. Dyke, M.K. Sain, J.D. Carlson, Journal of Engineering Mechanics 123 (1997) 230–238.
[5] J.D. Carlson, M.J. Chrzan, F.O. James, US Patent 5,284,330, 1994.
[6] J.D. Carlson, M.J. Chrzan, US Patent 5,277,281, 1994.
[7] W.H. Li, H. Du, G. Chen, S.H. Yeo, N.Q. Guo, Smart Materials & Structures 11 (2) (2002) 209–217.
[8] T. Shiga, A. Okada, T. Kurauchi, Journal of Applied Polymer Science 58 (1995) 787–792.
[9] M.R. Jolly, J.D. Carlson, B.C. Munzo, T.A. Bullions, Journal of Intelligent Material Systems and Structures 7 (1996) 613–622.
[10] W.M. Stewart, J.M. Ginder, L.D. Elie, M.E. Nichols, US Patent 5,816,587, 1998.
[11] J.R. Watson, US Patent 5,609,353, 1997.
[12] J.D. Carlson, M.R. Jolly, Mechatronics 10 (2000) 555–569.
[13] J.M. Ginder, M.E. Nichols, L.D. Elie, S.M. Clark, Proceedings of SPIE 3985 (2000) 418–425.
[14] J.M. Ginder, M.E. Nichols, L.D. Elie, J.L. Tardiff, Proceedings of SPIE 3675 (1999) 131–138.
[15] M. Lokander, B. Stenberg, Polymer Testing 22 (2003) 245–251.
[16] L.C. Davis, Journal of Applied Physics 85 (6) (1999) 3348–3351.
[17] X.Z. Zhang, X.L. Gong, P.Q. Zhang, Journal of Applied Physics 96 (4) (2004) 2359–2364.
[18] C.P. Jiang, Y.K. Cheung, International Journal of Solids Structures 35 (30) (1998) 3977–3987.